

# Adaptive degenerate space method for source term estimation using a backward Lagrangian stochastic model

O.Buchman<sup>1</sup>, E.Fattal<sup>1</sup>

<sup>1</sup>Applied Mathematics Department,  
Israel Institute for Biological Research, Ness Ziona, Israel

## Key Points:

- Source term estimation
- Backward Lagrangian stochastic model
- Formulation and analysis of degeneracy in phase space
- Optimal design

arXiv:2004.06526v1 [physics.comp-ph] 13 Apr 2020

---

Corresponding author: Omri Buchman, [omrib@iibr.gov.il](mailto:omrib@iibr.gov.il)

Corresponding author: Eyal Fattal, [eyalf@iibr.gov.il](mailto:eyalf@iibr.gov.il)

## Abstract

The general problem of characterizing gas source parameters based on concentration measurements is known to be a difficult task. As many inverse problems, one of the main obstacles for accurate estimation is the non-uniqueness of solution, induced by the lack of sufficient information. As the number of detectors is lowered, which is more than a plausible scenario for many practical situations, the number of possible solutions that can characterize the source increases dramatically, leading to severe errors. In this paper, a Lagrangian stochastic based method for identifying these suspected points, which will be referred to as 'degenerate space', is formulated and analysed. Then, a new procedure for quantitative prediction of the effect of deploying a new detector in space is used to design an adaptive scheme for source term estimation. This scheme has been tested for several scenarios, differing by the location of the initial detectors, and is shown to reduce dramatically the degeneracy formed by insufficient information. The combined formulation of degenerate space with the new adaptive scheme is shown to give improved accuracy, and in particular for a relatively small number of detectors.

## 1 Introduction

Solving the source estimation problem, i.e. identifying the source position and emission rate based on a given set of measurements, has great importance for many practical situations. For example, estimating the source parameters is a crucial preliminary step for applying a dispersion model in the process of risk assessment of biological or chemical release, as well as for identifying the source in accidental releases in industrial areas. Yet, despite its importance, solving the problem is a daunting task. One of the main reasons for this failure is that as many inverse modeling problems, the determination of source parameters from measurements is known to be an ill-posed problem, i.e the solution may not exist, may not be unique or suffers from discontinuity.

In the past twenty years a significant progress has been made in the development and testing of new methodologies for solving the source estimation problem, and in some cases truly remarkable results were obtained. A detailed review on possible methodologies for solving this problem is beyond the scope of this paper, and can be found in other places (Hutchinson et al., 2017). It should be noticed however, that in many cases, the number of detectors used is large for a rather small regime of interest. For example, Keats and Yee (A. Keats et al., 2007) combined the backward (adjoint) dispersion model into the Bayesian inference framework, to estimate the source position and intensity of a source in the well-known Mock Urban Setting Trial. Kumar (Kumar et al., 2015) applied the Regularization procedure for the same experimental data. Both authors managed to retrieve the source accurately, but the source estimation procedure relies on many detectors positioned in an area of  $200m \times 200m$ .

Clearly, adding more information by increasing the number of detectors will gradually solve the problem of non-uniqueness. While the validity of this statement is correct in general, its details are still unknown. For example, how many detectors are actually required in a certain scenario in order to obtain a reasonable accuracy? Are there any preferred locations for the detectors, and can they be predicted before or along the process of source estimation? These questions are crucial for both theoretical and applicative reasons, since the deployment of many detectors for covering a wide regime of interest may not be feasible. More than that, even for a relatively dense array of detectors, since both the source and the wind regime are unknown, measuring a significant concentration (above threshold) in a small number of detectors, is a plausible scenario.

Answering these questions can be related to the relatively new area of source term estimation using mobile sensors. This field seems to be very promising, since in principle, it allows to spare the need of pre-deployment of a dense array of detectors. More than that, the mobility of the detectors enables the possibility to update the position of the detectors along the process, in order to maximize the expected information gained by the measurements.

Ristic (Ristic et al., 2014) developed such an algorithm for the estimation of a radiological point source in the framework of Bayesian inference, where the detectors position update is chosen to maximize the expected information gain. While this idea seems to be very powerful for locating a radiological source, its extension to gas source is not trivial, since a closed formed expression for the dispersion model dependency on the source parameters is hard to obtain. Keats(W. A. Keats, 2009; A. Keats et al., 2010) applied the Bayesian adaptive exploration (BAE) methodology(Lindley, 1956; Loredo, 2004), which provides a way to decide how future experiments should be performed so that information about the phenomenon of interest is maximized, to add a new detector to an existing array of detectors deployed according to the original layout in the prey grass project.

In this paper, a new method for estimating both continuous and instantaneous source parameters is described. Based on that, a new mechanism for adaptive deployment of detectors along the process of source estimation of continuous source will be presented, which is designed to reduce the non-uniqueness of the problems solution. More specifically, we shall address the following issues:

1. Formalizing the degenerate space for a given set of measurements by identifying all suspected points in the parameter space which has approximately the same probability for characterizing the source. In section 2.2 a simple and efficient method will be presented, upon which our source estimation method is defined.
2. Based on the available measurements, a criterion for choosing a location for a new detector will be presented in section 2.3, aimed to reduce the effect of non-uniqueness by a statistical evaluation of the expected degeneracy reduction.
3. Based on the above two points, an iterative algorithm will be presented, which exploits the given information from a set of old measurements to plan the next measurement. The algorithm seems to converge fast, sparing the need for a large number of pre-deployed detectors, as will be shown in section 3.3.

## 2 Theory

### 2.1 The Lagrangian stochastic model

In order to solve the source estimation problem, one has to specify the underlying turbulent pollutant dispersion model. In this work, a Lagrangian stochastic model (LSM) developed at IIBR (Fattal, 2014), has been used. This modelling approach is known to be able to describe consistently gas dispersion phenomena, in rather complicated atmospheric scenarios such as non-homogeneous turbulent regimes, complex terrain and canopies (urban and vegetation). The LSM has been described in detail in many articles (Thomson, 1987; Wilson & Sawford, 1996). Briefly, the basic idea is to propagate the position and velocity of the Lagrangian fluid particles according to the Langevine equations:

$$dx_i = u_i dt \tag{1}$$

$$du_i = a_i(x, u, t)dt + b_{ij}(x, u, t)dW_j(t) \tag{2}$$

where  $x$  and  $u$  are the position and velocity of the particles and  $dW_i$  is a random increment selected from a Normal Distribution with variance  $dt$ . The deterministic coefficients  $a_i$  can

be determined via the Fokker-Planck equation, by satisfying the well mixed (necessary) condition (Thomson, 1987). According to the Kolmogorov similarity theory (Pope, 2000), the stochastic term takes the form of  $b_{ij} = \sqrt{(C_0\epsilon)}\delta_{ij}$  where  $\epsilon$  is the average dissipation rate of the kinetic energy.

By counting all touchdowns of the stochastic particles in some volume which represents the detector, one can calculate the probability density  $P^f(r, t|r', t')$  that a particle spreads from  $r'$  at time  $t'$  will reach the detector located at point  $r$  after time  $t$ . Flesch and Wilson (Flesch et al., 1995) showed that by modifying the Langevine equation, one can propagate the particles backwards in time (BLSM), i.e. from the future to the past, and that for an incompressible fluid the following relation holds:

$$P^f(r, t|r', t') = P^b(r', t'|r, t) \quad (3)$$

where  $P^b(r', t'|r, t)$  is the probability density function that a particle evolving from the detector located at  $r$  and propagated backwards in time, will reach the 'source' located at point  $r'$  at time  $t'$ .

The transition probability for such a process can be related to the ensemble averaged concentration (Flesch et al., 1995; Sawford, 1985) by:

$$d(r, t) = \int_0^\infty \int S(r', t') P^f(r, t|r', t') dt' dr' \quad (4)$$

where  $S(r', t')$  describes the spatial and temporal source distribution in  $kg \times m^{-3} \times sec^{-1}$ . The calculated concentration, averaged over the detector's volume  $v_d$  which is centered at position  $r$ , at stationary turbulence and sustained uniformly distributed source can be written as:

$$d(r) = \frac{q}{V_d} \int_{v_d} \left( \int_{v_s} \int_0^\infty P^f(r, t|r', 0) dt dr' \right) dr \quad (5)$$

where  $q$  is the emission rate,  $v_d$  is the volume of the detector and  $v_s$  is the volume of the source.

The parameter space  $\Theta$  will be discretized by setting a grid of  $N_x \times N_y \times N_q$  cells. Each hypothesis about the source will be labeled as  $\theta_j = (r_j, q_j) \in \Theta$ , where  $r_j = (x_j, y_j)$  and  $q_j$  are the coordinates of the center of the  $j$ th cell. Therefore the concentration at the  $i$ th detector, located  $R_i$  due to a source characterized by the  $j$ th hypothesis is given by:

$$d(R_i|\theta_j) = \frac{q_j}{V} \int_{v_i} \left( \int_{v_j} \int_0^\infty P^f(r, t|r', 0) dt dr' \right) dr = \frac{q_j}{V} \int_{v_j} \left( \int_{v_i} \int_0^\infty P^b(r', 0|r, t) dt dr \right) dr' \quad (6)$$

where  $v_j$  is the  $j$ th cell in the parameter space and  $v_i$  is a small volume centered on  $R_i$ . The last passage in 6, due to the Forward-Backward relation, can be very useful, as will be seen later.

## 2.2 Construction of the degenerate space

Suppose that there are  $M$  measurements of concentration  $d_1 d_M$  from detectors deployed at  $R_1 R_M$  correspondingly. For every measurement, if the dispersion model is correct and there is no measurement error or stochastic fluctuation, the source must be characterized by a hypothesis  $\theta_j$  for which  $d(R_i|\theta_j) = d_i$ . Now, by adding a stochastic noise to the calculation and measurement error, the reasonable range for every candidate hypothesis will be broadened. Therefore for every detector its corresponding iso-surface can be defined as:

$$A_i = \{\theta_j \in \Theta || d(R_i|\theta_j) - d_i | \leq \sigma\} \quad (7)$$

where  $\sigma$  describes the total discrepancy between the measured and calculated concentrations. The source must be contained in every iso-surface, but other points may also be included. Since this argument holds for all detectors, the source must be contained in their intersection. Therefore, based on  $M$  detectors measurements, define:

$$S(R_1 \dots R_M) = \bigcap_{i=1}^M A_i \quad (8)$$

as the degenerate space, i.e. all the points in the parameter space which can serve as a reasonable hypotheses for characterizing the source. In practice, the calculation of the degenerate space using the forward LSM is not practical, since from every point in the parameter space an independent operation of the LSM model is required. Then, only if the concentration at every detector will fulfill the criterion of equation 7, the point should be included in the corresponding iso-surface. There is, however, a significant shortcut which makes this procedure not only possible but almost immediate the use of the BLSM instead of the LSM as the dispersion model. By substituting equation 6 in equation 7 one gets:

$$A_i = \left\{ \theta_j \in \Theta \left| \frac{q_j}{V} \int_{v_j} \left( \int_{v_i}^{\infty} P^b(r', 0 | r, t) dt dr' \right) dr' - d_i \right| \leq \sigma \right\} \quad (9)$$

Note that for a given detector, the calculation of the integral in the last expression for all hypotheses can be done with the same BLSM operation. Hence, the number of required BLSM operations is equal to a total number of detectors, rather than the number of hypotheses, leading to a dramatic reduction in the required computational effort (the same idea makes the BLSM so efficient for source estimation in the first place).

Detectors which measured a zero concentration also contribute valuable information, since they eliminate parts of the space for the source position. Therefore we can define another type of iso-surface:

$$B_i = \{ \theta_j \in \Theta | |d(R_i | \theta_j) - d_{th}| > \sigma \} \quad (10)$$

where  $d_{th}$  is the detector threshold. The degenerate space can be modified as:

$$S(R_1 \dots R_M) = \bigcap_{d_i > 0}^M A_i \setminus \bigcup_{d_i = 0}^M B_i \quad (11)$$

A demonstration of this idea can be seen in Figure 1. In the left panel, the forward dispersion map from a source located at  $x_s = 5000, y_s = 5000$  with an emission rate of  $q_s = 1 \text{ kg/min}$  and an average uniform wind speed of  $2 \text{ m/sec}$  is shown. This calculation was then used to generate the input concentration for four detectors, designated as black points on the plot. Note that the concentration at the two right detectors is above threshold, and zero in the two left detectors. Based on these measurements, the corresponding iso-surfaces were calculated, assuming that the emission rate is known as can be seen in the right panel. The intersection of the two non-zero concentration iso-surfaces ("A type iso-surfaces", see equation 7) contain two clusters of points, designated by orange points in the figure. The contribution of measurements below the detectors threshold ("B type iso-surfaces", see equation 10) can be seen in shade gray on top of the intersection mentioned before. One can see that the addition of this information rules out the artifact cluster, leaving only the correct center included in the degenerate space.

The non-uniqueness of the solution might have a severe effect on the ability to characterize the source correctly. To see that, we shall briefly describe two fundamental approaches to source estimation. A standard approach for solving the source estimation problem is to seek for the hypothesis which minimizes a cost function which compares the measured and the calculated concentration at all detectors. A commonly used cost function (Hutchinson et al., 2017) is the square of differences  $\chi^2 = \sum_{i=1}^M \frac{(d(R_i | \theta) - d_i)^2}{\sigma_i^2}$ . Since the degenerate points

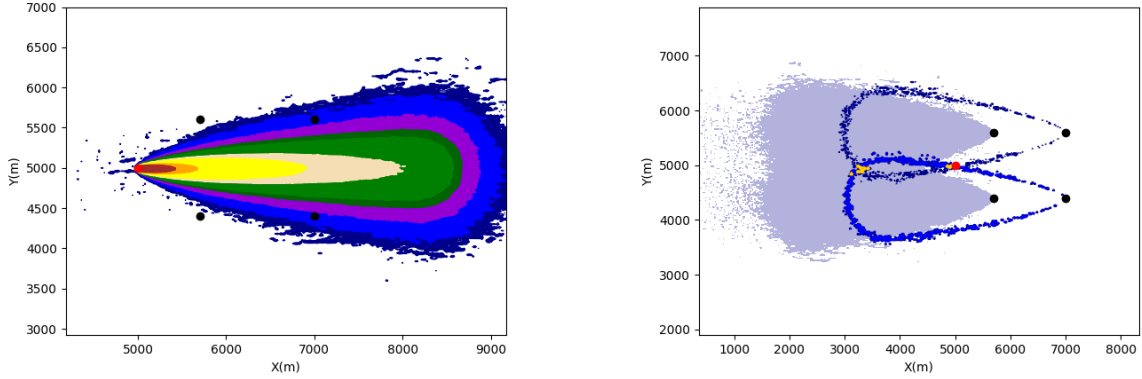


**Figure 1.** An example of the iso-surfaces method for the construction of the degenerate space is shown. In the left panel the concentration map formed from a source located at 5000, 5000 is shown. Four detectors were used for the source estimation, but only two of them measured concentration above threshold. Two clusters of degenerate points are formed by the intersection of these two iso-surfaces, as can be seen in orange dots in the right panel. The grey area, which represents the forbidden regime formed by the other two detectors, eliminates one of the clusters in the degenerate space, leaving only the cluster surrounding the actual source location.

cannot be differentiated by this cost function, if the degenerate space is large and sparse a severe instability of the algorithm will be obtained. For example, in the previously mentioned case, if only the two left detectors are available the degenerate space will contain two clusters of points centered on (5000, 5000) and (3300, 5000). Hence, by minimizing  $\chi^2$  the source estimation has the same probability to have either a small error or a very large error (1700m).

In the past few years, the estimation of the source parameters in the framework of Bayesian inference became very popular (A. Keats et al., 2007; Yee, 2008, 2012; Yee et al., 2014; Hazart et al., 2014; Xue et al., 2017). Briefly, the basic idea is to construct the posterior distribution  $P(\theta|D)$ , which describes the probability that a certain hypothesis will be correct based on a given set of data  $D$ . By using Bayes theorem and without prior knowledge, this function can be written as:

$$P(\theta|D) \propto e^{-\chi^2} \quad (12)$$

The source estimation can be derived from the posterior distribution, either by locating the hypothesis which maximizes the distribution, or by sampling it in order to calculate some related averages such as its moments. Either way, the instability induced by degeneracy which characterized the minimization of the cost function in equation (10) cannot be avoided by using the Bayesian inference approach.

### 2.3 Adaptive degeneracy reduction

Adding a new detector to the system will reduce the degeneracy formed by the lack of sufficient information. An interesting question rises based on the current information, gained by the available measurements, where should a new detector be deployed? In terms of degeneracy, a good measurement is one for which a large reduction occurred, a bad measurement leaves the degenerate space approximately in the same size and shape. In this section a mechanism for answering this question will be presented. Recall that all the points for which

$$|d(R_i|\theta_j) - d_i| \leq \sigma(d(R_M|\theta_i), d_i) \quad (13)$$

for all  $i = 1 \dots M$ , can be regarded as reasonable candidates for describing the source. The total error is composed by the model fluctuations  $\sigma_c(d(R_M|\theta_i))$  and measurement error  $\sigma_m(d_i)$  (the subscripts c and m refer to calculated and measured concentrations respectively). In principle, the dependency of both errors with their corresponding concentrations has to be modeled. For the rest of this paper, we shall assume that the detector's error can be neglected (which is reasonable if the concentration is averaged over a relatively long time), or has no explicit dependency on the measured value, so:

$$\sigma(d(R_i|\theta_j), d_i) = \sqrt{\sigma_c^2(d(R_i|\theta_j)) + const} \quad (14)$$

The functional form of the stochastic error will be discussed in section 3.1. The degenerate space, as defined in equations 8 and 11, did not assume any preference between the degenerate points contained within it. Hence, all the degenerate points have the same probability for characterizing the source, i.e:

$$\forall \theta_j \in S(R_1 \dots R_M) P(\theta_j) = \frac{1}{|S(R_1 \dots R_M)|} \quad (15)$$

Next, define the degenerate space if the source is fully characterized by  $\theta_i$  as:

$$S(R_1, \dots, R_{M+1}|\theta_i) = \{\theta_k \in S(R_1, \dots, R_M) \mid |d(R_{M+1}|\theta_k) - d_{M+1}| \leq \sigma(d(R_{M+1}|\theta_k))\} \quad (16)$$

where  $d_{M+1}$  is the concentration that will be measured at the new detector, positioned at  $R_{M+1}$ . The reduction factor after the new measurement occurred is defined as:

$$\Gamma(R_1, \dots, R_{M+1}|\theta_i) = \frac{|S(R_1, \dots, R_{M+1}|\theta_i)|}{|S(R_1, \dots, R_M)|} \quad (17)$$

Since all the hypotheses have the same probability for describing the source, a simple solution for the problem could be to deploy the new detector at a point which maximizes the probability (over  $S(R_1, \dots, R_M)$ ) that for a random choice of  $\theta$  the reduction factor will be small. This procedure is not possible however, since the reduction factor can be determined only after the new detector has been deployed and the concentration measurement has occurred, a data which is not attainable at the current stage. Therefore, we define an estimator for the reduction factor as:

$$\gamma(R_1, \dots, R_{M+1}|\theta_i) = \frac{|s(R_1, \dots, R_{M+1}|\theta_i)|}{|S(R_1, \dots, R_M)|} \quad (18)$$

where  $s(R_1, \dots, R_{M+1}|\theta_i) =$

$$\{\theta_k \in S(R_1, \dots, R_M) \mid |d(R_{M+1}|\theta_k) - d(R_{M+1}|\theta_i)| \leq \sigma(d(R_{M+1}|\theta_k)) + \sigma(d(R_{M+1}|\theta_i))\} \quad (19)$$

Now, Let's relate  $\Gamma(R_1, \dots, R_{M+1}|\theta_i)$  to  $\gamma(R_1, \dots, R_{M+1}|\theta_i)$ . By definition, for every  $\theta_k \in S(R_1, \dots, R_{M+1}|\theta_i)$  the following inequality holds:

$$|d(R_{M+1}|\theta_k) - d_{M+1}| \leq \sigma(d(R_{M+1}|\theta_k)) \quad (20)$$

In addition, since we assumed that  $\theta_i$  is the correct hypothesis, we get:

$$|d(R_{M+1}|\theta_i) - d_{M+1}| \leq \sigma(d(R_{M+1}|\theta_i)) \quad (21)$$

The combination of these inequalities leads to

$$|d(R_{M+1}|\theta_i) - d(R_{M+1}|\theta_k)| \leq \sigma(d(R_{M+1}|\theta_i)) + \sigma(d(R_{M+1}|\theta_k)) \quad (22)$$

So  $\theta_k \in s(R_1, , R_{M+1})|\theta_i$ . Therefore we showed that:

$$S(R_1, , R_{M+1})|\theta_i \subseteq s(R_1, , R_{M+1})|\theta_i \quad (23)$$

which implies that for every  $\theta_i$ :

$$\Gamma(R_1, , R_{M+1})|\theta_i \leq \gamma(R_1, , R_{M+1})|\theta_i \quad (24)$$

Since all points have the same probability for characterizing the source, the probability that for a random choice of hypothesis the estimator will be smaller than some small number  $\alpha$  can be calculated as

$$P(\gamma(R_1, , R_{M+1}) \leq \alpha) = \frac{|\{\theta_i|\gamma(R_1, , R_{M+1})|\theta_i \leq \alpha\}|}{|S(R_1, , R_M)|} \quad (25)$$

Therefore a reasonable approach may be to seek for the location which maximizes this expression

$$e = \arg \max_{R_{M+1}} P(\gamma(R_1, \dots, R_{M+1}) \leq \alpha) \quad (26)$$

for a small value of  $\alpha$ , specified by the user. Furthermore, equation 24 implies that for the preferred position if  $P(\gamma(R_1, , e) \leq \alpha) = \beta$  then:

$$P(\Gamma(R_1, , e) \leq \alpha) \geq \beta \quad (27)$$

Clarification of the last claim can be seen by the following example: assume that we have 100 points and we obtain  $P(\gamma(R_1, , e) \leq 0.2) = 0.6$ . Therefore, there are 60 points for which  $\gamma(R_1, , e|\theta_i) \leq 0.2$  and for 40 points  $\gamma(R_1, , R_e|\theta_i) > 0.2$ . For each point of the first class we have  $\Gamma(R_1, , e|\theta_i) \leq \gamma(R_1, , e|\theta_i) \leq 0.2$  so the probability that  $P(\Gamma(R_1, , e) \leq 0.2) \geq 0.6$ .

What is the meaning of this criterion? equation 27 ensures that the probability that the reduction factor is smaller than a chosen  $\alpha$  is larger than the optimized  $\beta$ . For the rest of the paper, we shall use  $\alpha = 0.2$ , meaning that the reduction of degenerate space is at least by factor 5. As we shall see later, in many cases the probability for such a reduction will be larger than 0.6.

So far, two types of operations have been mentioned the reduction of degeneracy by measurement and a proposition for a new detectors position. These operations can be combined into an iterative procedure, where in every cycle, the degeneracy of the previous step is used to deploy the new detector. A schematic description for such algorithm is:

while  $N_d > toll$  :

1. Prediction: based on  $S(R_1 R_M)$ , use equation 26 to estimate  $e$
2. Measurement: deploy the new detector at  $e$  and measure  $d_{M+1}$
3. Reduction: use the new data to construct the new degenerate space  $S(R_1 R_M, e)$
4. Calculate  $N_d = |S(R_1 R_M, e)|$  and repeat step 1

where  $toll$  and  $\alpha$  have to be specified by the user and  $N_d$  is the number of degenerate points.

### 3 Results

#### 3.1 Numerical details

in this section both the iso-surface crossing method for construction of degenerate space and the adaptive source term estimation will be examined. In all cases the emission rate is 1 kg/min and the external wind is 2 m/sec in the east direction in neutral stability. Unless mentioned otherwise, the source is located at the center of  $10km \times 10km$  grid composed by cells of  $20m \times 20m$ . The Lagrangian stochastic model is used to calculate the concentration based on 400000 Lagrangian particles.

The construction of the degenerate space at each cycle requires the specification of the stochastic noise dependency on the calculated concentration. In order to estimate this relation a series of 30 identical LSM operations was performed, differing by their random seeds. Based on these calculations, the ratio between the standard deviation and the average concentration was calculated at 7 typical points located downstream to the source position. This ratio, averaged over these points, is  $0.15 \pm 0.14$ , so  $\sigma_c = 0.3 \times d$  can serve as an upper bound for the correct standard deviation.

Note that taking a bit broader value for the standard deviation is not a major problem, since the fictitious points that may be included by it could be removed by the adaptive mechanism. On the other hand, taking a smaller value than the correct one might cause a serious problem, since recovering a good point which was accidentally rejected is impossible.

#### 3.2 Features of the degenerate space

We shall start the discussion on the structure of the degenerate space in the relative simple case where the emission rate is known a priori and the objective of the algorithm is locating the source position only. In the first 6 panels of Figure 2 the union and intersection of two detector's iso-surfaces is shown for several configurations of the detectors. In all cases the degenerate space is composed of either one or two relatively compact clusters of points in the close surrounding of the two iso-surfaces intersections. Intuitively, these results can be generalized to many cases as long as the wind is not too far from homogeneous. Clearly, adding detectors will constantly improve the result of the algorithm. But the last result implies that the contribution of a new detector will be more dramatic if it will exclude a whole cluster of degenerate points, as can be seen in the lower right case in figure 2. Therefore we expect that in most cases, the contribution of the third detector will be much larger than all other detectors to follow. This type of behavior can be seen in figure 3, where the error in of the source estimation output can be seen for 1 to 4 detectors as a function of a number of particles. One can see that for every number of detectors, the error stabilized on a certain level as the number of particles grows, but this numerically converged value drops dramatically as the number of detectors increases from 2 to 3, and much less as going from 3 to 4 detectors.

Now, lets return to the general problem where both the emission rate and source location is unknown where only two detectors are available. The absence of knowledge about the source emission rate increases dramatically the dispersion of degenerate points since there are many more combinations of the three parameters that yields the same concentration at the pre-deployed detectors. Two examples of the degenerate space formed by two detectors can be seen by the blue points in the upper right panels of figures 5 and 6, differing by the locations of the two detectors (the locations of the two detectors can be seen as the black and cyan pair of points in Figure 4). Note that the degenerate points are relatively spread in the parameter space, so simple averaging will lead to severe errors in approximating the source.

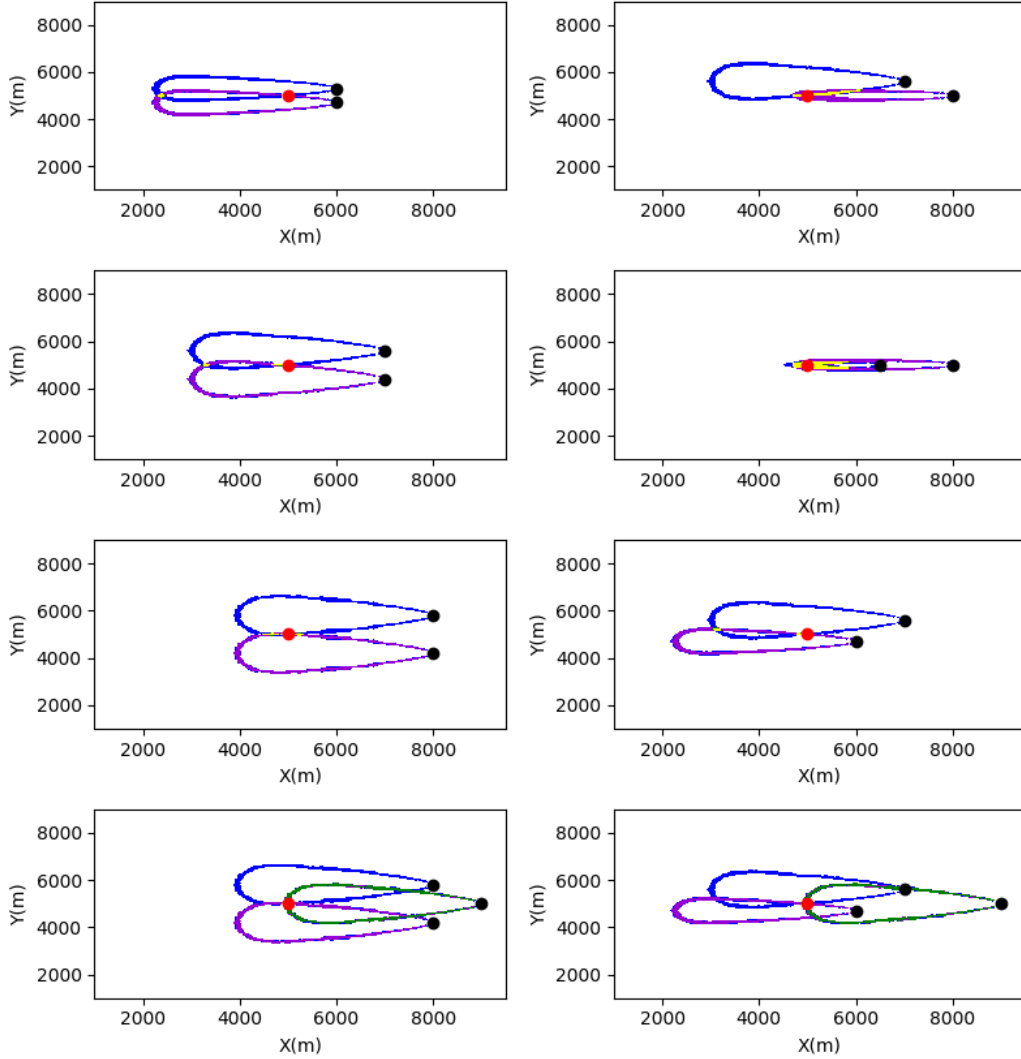


**Figure 2.** The degenerate space, formed by an iso-surfaces intersection, is shown for 8 cases differing by the number of the detectors (2 detectors in the first six cases and 3 detectors in the last two cases) and their arrangement. In all cases there are at most two clusters of degenerate points, centered along the intersections of the corresponding iso-surfaces. The effect of adding a third detector can be seen by comparing the third and fourth rows either eliminating a whole cluster (right panels) or significant reduction of the cluster, if only one cluster exists (left panel).

### 3.3 Testing the adaptive source algorithm

We shall examine the adaptive source term estimation algorithm, specified in section 2.3, in six cases differing by the initial arrangement of the first two pre-deployed detectors and the source location. The concentration map generated by operating the Lagrangian stochastic model for source located at (5000, 5000), is shown in Figure 4. A different color is used to designate the pair of detectors of the first four cases. In the first case (black points) the first two detectors are pre-deployed along the same line parallel to the wind direction. In the second case (yellow points) the detector aligned the same line perpendicular to the external line. In cases 3 (green) and 4 (cyan) the symmetry was removed. In the last two

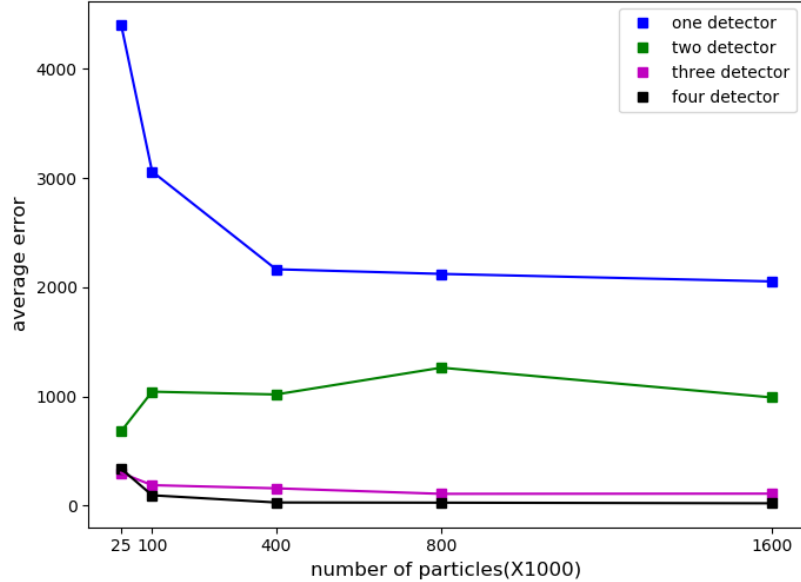


**Figure 3.** The convergence of the error in the estimation of the source position is shown as a function of a number of particles for a different number of detectors (the location of the first two detectors corresponds to the third case in Figure 2). A dramatic improvement can be seen by adding a third detector, induced by the elimination of a whole cluster of degenerate points. Adding a fourth detector slightly improves the converged error by further reducing the remaining cluster of points.

cases, which are not displayed in the Figure, the detectors locations' are the same as the fourth case, but the source is located at (4000, 5200) and (4200, 4800) correspondingly. In all cases the input concentration for the source estimation process was taken as the value of the map at the detectors positions. Full analysis cases 1 and 4 can be seen in Figures 5 and 6 and shall now be described.

**Case 1:** In the upper-right panel of Figure 5, a map of  $P(\gamma(R_1, R_2, R_3) \leq 0.2)$  as a function of  $R_3$  is shown, based on the available measurements at the first two detectors located at  $R_1 = (6500, 5000)$ ,  $R_2 = (8000, 5000)$  (also shown as black crosses on the map). One can easily obtain two stretches of preferred points and a wide un-preferred regime enclosed by these two stretches. The position of the third detector was chosen at (6000, 5300) for which the criterion is maximized. The effect of this choice on the degeneracy reduction can be seen in the upper right panel of Figure 5. The degenerate space before and after the third measurement can be seen in blue and black points correspondingly. Note that the wide and spread original space that contained 8100 points, has been reduced to a narrow diagonal stretch containing only 1023 points.

The first row in figure 5 describes the first cycle in the operation of the adaptive algorithm for case 1. The next row can be understood in a similar way in the left panel a map of the predicted reduction is formed based on the degenerate space of the previous iteration (note that a new black cross was added at the optimized position of the previous cycle), and a point which optimizes this map is chosen as the position of the new (fourth) detector. The effect of the new measurement can be shown in the right panel in the second row. As before, blue points represent the degenerate space before the addition of the new detector, which is the outcome of the last cycle, and black points represent the remaining points after the

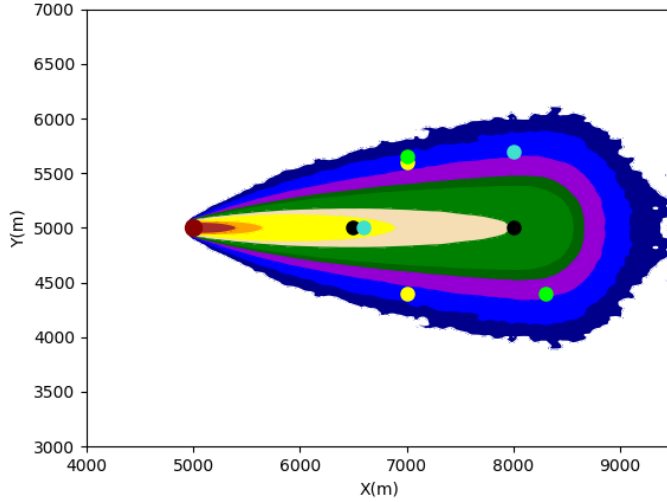


**Figure 4.** The concentration map, generated by a source located at  $(5000m \times 5000m)$  is shown. The position of the two detectors for the first four cases are also shown, each case represented by a different color (black for case 1, yellow for case 2, green for case 3 and cyan for case 4)

addition of the new information.

Note that the initial arrangement of the detectors along a line parallel to the wind direction, led to a very large and spread initial degenerate space. Nevertheless, every addition of detector reduces dramatically the size and shape of the degenerate space of the last cycle, so after deployment of two new detectors, the degenerate space is condensed in the small proximity of the source, represented by the red dot in the lower right panel.

The performance of the adaptive algorithm along three cycles (the third cycle is not shown in Figure 5) for the first case are summarized in the upper part of table 1. For each cycle the number of degenerate points, as well as the averaged source parameters and their corresponding standard deviations are shown (the actual source position and emission rate were subtracted from the averages). One can clearly see fast convergence in all these criteria to the correct value.

**Case 4:** In Figure 6, a similar analysis for the fourth case (cyan dots in Figure 4) is shown. The asymmetric deployment of the first two detectors dictates an asymmetric shape of the probability map. In addition, the regime of high probability is far more narrow and difficult to predict intuitively without a detailed calculation. In this case, the initial averages and standard deviations of all parameters are large, as can be seen in the first row of case 4 in table 1. Adding new detectors dramatically reduces the error of all parameters, as can be seen in the following rows of the table, as well as by comparing the blue and black points in the figure.

A summary of all six cases is presented in table 1. The number of cycles is limited by the demand that the number of degenerate points is less than 30 points. As mentioned before, the search was done in parameter space of  $10000m \times 10000m$ , so the relative error of every spatial parameter, normalized by the corresponding length scale, in the end of the algorithm operation is very small. More than that, the resolution of the source estimation is limited by the size of the grid cells used to predict the concentration from the LSM operation, which is  $20m \times 20m$  in these cases. Therefore, in all cases, the errors are within deviation of three cells at the most.

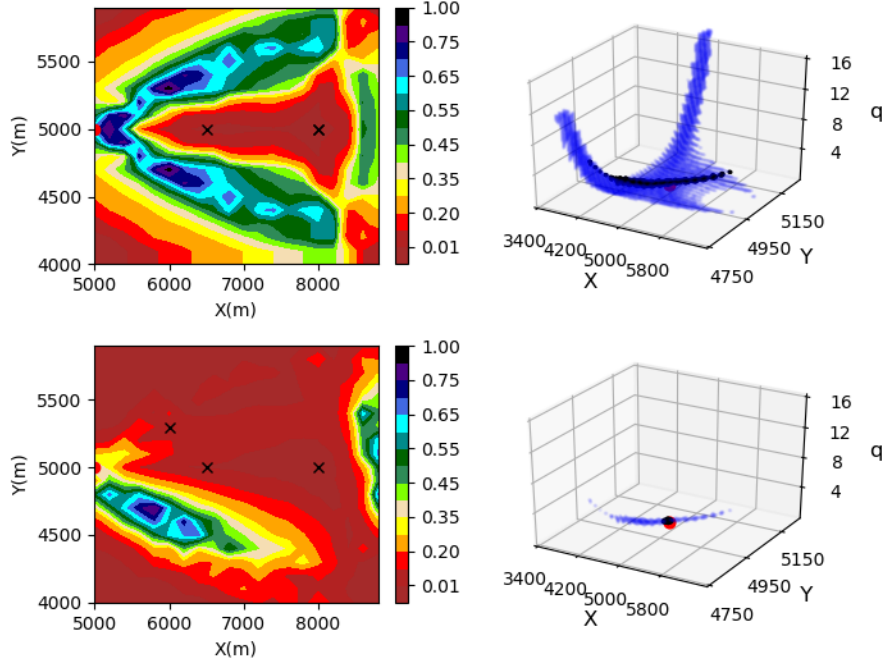


**Figure 5.** Case 1 analysis: Each row describes a cycle of the algorithm, starting from two detectors located at  $(6500, 5000)$  and  $(8000, 5000)$ . In the left side of each row, the expected reduction according to the criterion described in equation 26 is shown for all possible locations of the new detector. The already deployed detectors, used for the construction of the degenerate space in the beginning of the cycle, are designated by black crosses. The degenerate space before (blue) and after (black) the deployment of the new detector can be seen in the right panel of every row. The actual reduction gained by the procedure can be seen by the difference between the two colors. After two cycles, the degenerate space is reduced almost entirely to the correct source parameters, represented by the red dot.

## 4 Summary and Discussion

In this paper we have presented a general new approach for source term estimation, which is built to minimize the problem of degeneracy—the existence of many hypotheses with approximately the same probability for describing the source parameters. This adaptive approach relies on two concepts—the identification of the suspected points based on current measurements, and the prediction of the new detector’s position.

Identifying the suspected points, can be achieved by examining the intersection of the detectors corresponding iso-surfaces, as mentioned in section 2.2. This procedure is easy to apply and requires only one BLSM operation per detector. This idea is a bit similar in its character to the approach presented by Pudykiewicz (Pudykiewicz, 1998, 2007). Pudykiewicz noted that the source location must be contained in the intersection of all the supports of the influence functions, generated by solving the adjoint transport equation for every detector in the network. Based on that, he assigned a probability density function to this space, and considered the source location as its maximum. While the seeming resemblance, there are several differences between these approaches: first, the assigning of the probability density to the space, which led to some controversial discussions xxx in the literature, has not been assumed here. Second, to the best of my understanding, the

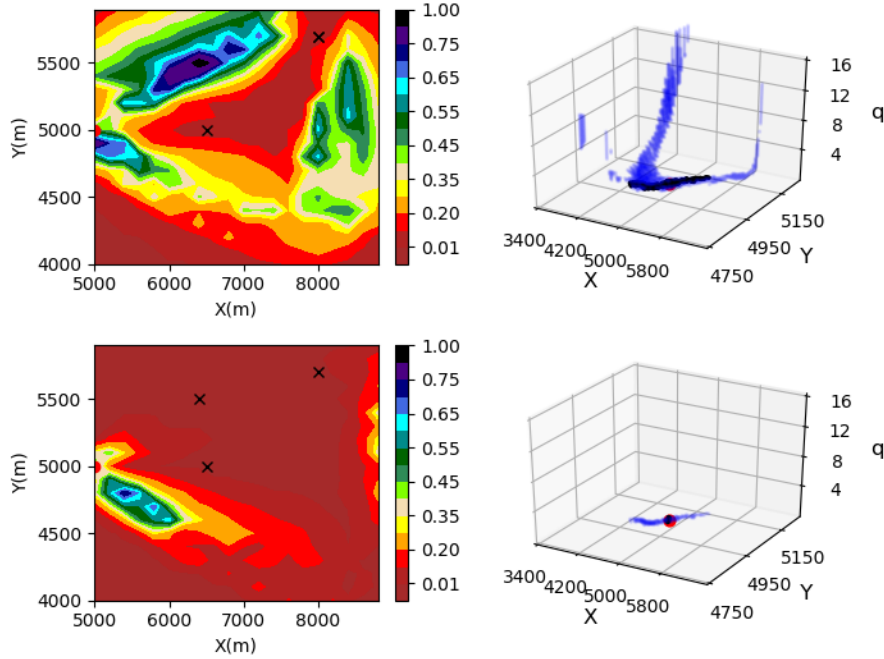


**Figure 6.** Case 4 analysis: the same analysis as described in the previous figure, starting from two detectors located at (6500,5000) and (8000,5700)

supports of the influence functions have no explicit dependency on the measured value of concentration in every detector, while the iso-surfaces in this paper have been tailed to fit the measured value.

Keats (A. Keats et al., 2007) demonstrated how the regimes of influences, generated by solving the adjoint diffusion-advection equation for every detector, can be used to select the possible locations of the source. Once again, these regime of influences, are taken as the solution of the adjoint equation for every detector ( $C^*$  which solves equation 16 in Keats paper), regardless of the concentration that was actually measured.

An important clarification has to be made about the proposition mechanism presented before. By no means, do we claim that the proposed location for the new detector will be the one that will maximally reduce the degeneracy after the measurement will occur. We simply claim that based on the available information at a certain cycle, it has a high probability for a significant reduction of degeneracy. Yet, one may ask in what sense the proposed location for the new detector is preferred over other possible propositions in space? To answer this, recall the situation described in first cycle of case 2. The degenerate space formed by two detectors located at (7000,5600) and (7000,4400) has 1795 points, and by construction, the source can be found at any one of these points. Based on that, the procedure described in section 2.3 predicted that  $e=(6000,5300)$  should be the position for the third detector.

The quality of this suggestion can be tested simply by "deploying" the detector at this point, measuring the concentration and reducing the degenerate space, compared to the same procedure for different candidates. It may seem a bit disappointing to note that there are other candidates for the new detector's position that will induce a larger actual reduction. This test is however misleading, since the measurement step relied on the knowledge of the source - in this case at (5000,5000,1). In practice all points in the degenerate space can serve as a source with the same probability - this is exactly how it was built. Repeating this procedure for a different source point, taken from the degenerate space, may lead to a completely different actual reduction.

**Table 1.** The results of the adaptive source estimation algorithm for six cases are shown in the table. For every case, the first row describes the features of degenerate space before applying the adaptive algorithm, based on two pre-deployed detectors. At every row, the number of degenerate points, the averages of the source parameters (after subtraction of the exact value) and their corresponding standard deviations are shown

cycle	$N_{detectors}$	$N_d$	$\langle x \rangle$	$\langle y \rangle$	$\langle q \rangle$	$\sigma_x$	$\sigma_y$	$\sigma_q$
CASE 1								
	2	8704	231	3.76	3.7	400	210	4.24
1	3	459	129	32	0.68	296	72	0.92
2	4	32	36	0	0.12	45	0	0.19
3	5	20	7	0	0.18	26	0	0.18
CASE 2								
	2	2160	877	0	3.6	1073	20	3
1	3	183	27	0.3	0.8	329	10.5	0.97
2	4	12	45	0	0.18	27	0.0	0.12
CASE 3								
	2	1920	26	67	3.9	630	139	3.1
1	3	65	39	11	0.21	74	12	0.25
2	4	28	28	13	0.06	41	13	0.15
CASE 4								
	2	3508	454	90	3.5	607	171	3.9
1	3	341	60	22	0.35	180	52	0.44
2	4	13	6	4	0.17	33	8	0.19
CASE 5								
	2	2462	437	2.8	3.5	768	102	3.11
1	3	212	120	4.8	0.21	191	19	0.25
2	4	89	62	6.9	0.02	80	17	0.14
CASE 6								
	2	624	973	160	1	946.9	186.8	1.3
1	3	62	33	25	0.5	64.6	43.5	0.8
2	4	7	6	3	0.1	14.0	7.0	0.2

Therefore a better criterion for estimating the quality of a candidate, may be to average the actual reduction over all degenerate points. For the preferred point, the average actual reduction factor is 0.12 and the standard deviation is 0.063.

This criterion can be used to compare the quality of the preferred point to arbitrary propositions for the third detector's position. In figure 7 the actual reduction factor, averaged over all degenerate points, is shown for arbitrary possible positions along the center lines  $(x, 5000)$  and  $(x, 5500)$ . For all cases, the averaged reduction factor is larger than for the preferred position (red point), and in most cases the value is about 0.3 - 0.4 with a standard deviation of 0.2 - 0.3, which is considerably higher than for the preferred position. Therefore a clever choice of the third detector position is crucial for source estimation, and the previously suggested proposition mechanism seems to predict correctly the effect of degeneracy reduction induced by the measurement.

### Acknowledgments

The authors would like to thank R. Baer for useful conversations and comments.

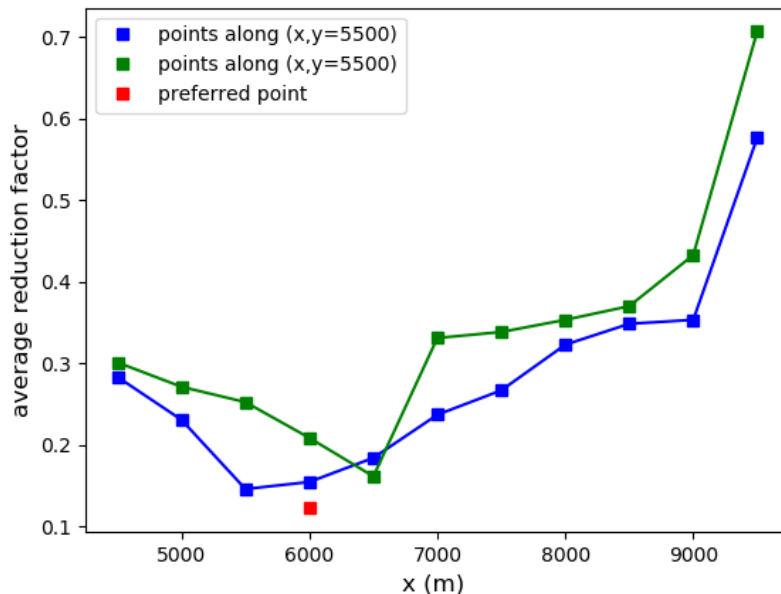


**Figure 7.** The actual reduction, averaged over all possible hypotheses in the first cycle of case 2, is shown for different points along the line  $(x,5000)$  and  $(x,5500)$ . Note that the best performance is achieved for the preferred point (red point).

## References

- Fattal, E. (2014). *A non-homogeneous non-gaussian lagrangian-stochastic model for pollutant dispersion in complex terrain, and its comparison to haifa 2009 tracer campaign* (IIBR Scientific Report, Nos. 2014/56/53/5614, Oct. 2014).
- Flesch, T. K., Wilson, J. D., & Yee, E. (1995). *Backward-time Lagrangian stochastic dispersion models and their application to estimate gaseous emissions* (Vol. 34) (No. 6). doi: 10.1175/1520-0450(1995)034<1320:BTLSDM>2.0.CO;2
- Hazart, A., Giovannelli, J. F., Dubost, S., & Chatellier, L. (2014). Inverse transport problem of estimating point-like source using a Bayesian parametric method with MCMC. *Signal Processing, 96*(PART B), 346–361. Retrieved from <http://dx.doi.org/10.1016/j.sigpro.2013.08.013> doi: 10.1016/j.sigpro.2013.08.013
- Hutchinson, M., Oh, H., & Chen, W. H. (2017). A review of source term estimation methods for atmospheric dispersion events using static or mobile sensors. *Information Fusion, 36*, 130–148. Retrieved from <http://dx.doi.org/10.1016/j.inffus.2016.11.010> doi: 10.1016/j.inffus.2016.11.010
- Keats, A., Yee, E., & Lien, F. S. (2007). Bayesian inference for source determination with applications to a complex urban environment. *Atmospheric Environment, 41*(3), 465–479. doi: 10.1016/j.atmosenv.2006.08.044
- Keats, A., Yee, E., & Lien, F. S. (2010). Information-driven receptor placement for contaminant source determination. *Environmental Modelling and Software, 25*(9), 1000–1013. Retrieved from <http://dx.doi.org/10.1016/j.envsoft.2010.01.006> doi: 10.1016/j.envsoft.2010.01.006
- Keats, W. A. (2009). Bayesian inference for source determination in the atmospheric environment.
- Kumar, P., Feiz, A. A., Singh, S. K., Ngae, P., & Turbelin, G. (2015). Reconstruction of an atmospheric tracer source in an urban-like environment. *Journal of Geophysical*

- Research*, 120(24), 12,589–12,604. doi: 10.1002/2015JD024110
- Lindley, D. V. (1956). On a Measure of the Information Provided by an Experiment. *The Annals of Mathematical Statistics*, 27(4), 986–1005. doi: 10.1214/aoms/1177728069
- Loredo, T. J. (2004). Bayesian Adaptive Exploration. , 330–346. doi: 10.1063/1.1751377
- Pope, S. B. (2000). *Turbulent Flows*. Cambridge University Press. doi: 10.1017/CBO9780511840531
- Pudykiewicz, J. A. (1998). Application of adjoint tracer transport equations for evaluating source parameters. *Atmospheric Environment*, 32(17), 3039–3050. doi: 10.1016/S1352-2310(97)00480-9
- Pudykiewicz, J. A. (2007). Comments on: "Bayesian inference for source determination with applications to a complex urban environment" by A. Keats, E. Yee, and Fue-Sang Lien. *Atmospheric Environment*, 41(26), 5541–5546. doi: 10.1016/j.atmosenv.2007.04.023
- Ristic, B., Skvortsov, A., & Walker, A. (2014). Autonomous search for a diffusive source in an unknown structured environment. *Entropy*, 16(2), 789–813. doi: 10.3390/e16020789
- Sawford, B. L. (1985). *Lagrangian statistical simulation of concentration mean and fluctuation fields*. (Vol. 24) (No. 11). doi: 10.1175/1520-0450(1985)024<1152:LSSOCM>2.0.CO;2
- Thomson, D. J. (1987). Criteria for the selection of stochastic models of particle trajectories in turbulent flows. *Journal of Fluid Mechanics*, 180(2), 529–556. doi: 10.1017/S0022112087001940
- Wilson, D. J., & Sawford, B. L. (1996). Review of Lagrangian stochastic models for trajectories in the turbulent atmosphere. *Bound.-Layer Meteorol.*, 78(1), 191–210.
- Xue, F., Li, X., & Zhang, W. (2017). *Bayesian identification of a single tracer source in an urban-like environment using a deterministic approach* (Vol. 164). Elsevier Ltd. Retrieved from <http://dx.doi.org/10.1016/j.atmosenv.2017.05.046> doi: 10.1016/j.atmosenv.2017.05.046
- Yee, E. (2008). Theory for reconstruction of an unknown number of contaminant sources using probabilistic inference. *Boundary-Layer Meteorology*, 127(3), 359–394. doi: 10.1007/s10546-008-9270-5
- Yee, E. (2012). Inverse Dispersion for an Unknown Number of Sources: Model Selection and Uncertainty Analysis. *ISRN Applied Mathematics*, 2012, 1–20. doi: 10.5402/2012/465320
- Yee, E., Hoffman, I., & Ungar, K. (2014). Bayesian Inference for Source Reconstruction: A Real-World Application. *International Scholarly Research Notices*, 2014(1), 1–12. doi: 10.1155/2014/507634